PHYSICAL REVIEW E **81**, 030104(R) (2010)

Bose-Einstein condensation in the Apollonian complex network

I. N. de Oliveira,[1] F. A. B. F. de Moura,[1] M. L. Lyra,[1] J. S. Andrade, Jr.,[2] and E. L. Albuquerque[3]
[1]*Instituto de Física, Universidade Federal de Alagoas, 57072-970 Maceió, AL, Brazil*
[2]*Departamento de Física, Universidade Federal do Ceará, 60451-970 Fortaleza, CE, Brazil*
[3]*Departamento de Física, Universidade Federal do Rio Grande do Norte, 59072-970 Natal, RN, Brazil*
(Received 7 January 2010; published 24 March 2010)

We demonstrate that a topology-induced Bose-Einstein condensation (BEC) takes place in a complex network. As a model topology, we consider the deterministic Apollonian network which exhibits scale-free, small-world, and hierarchical properties. Within a tight-binding approach for noninteracting bosons, we report that the BEC transition temperature and the gap between the ground and first excited states follow the same finite-size scaling law. An anomalous density dependence of the transition temperature is reported and linked to the structure of gaps and degeneracies of the energy spectrum. The specific heat is shown to be discontinuous at the transition, with low-temperature modulations as a consequence of the fragmented density of states.

DOI: 10.1103/PhysRevE.81.030104 PACS number(s): 05.30.Jp, 67.85.Jk, 64.60.aq, 89.75.Hc

The study of physical models embedded in complex networks has contributed to the understanding of transport and information flow within systems of many degrees of freedom [1–5]. Although many models have been proposed to describe real-life networks, most of them are stochastic models, presenting the disadvantage that fixed degree distributions are not constructed by recursive methods. Deterministic models have the strong advantage to often allow the possibility to compute analytically their properties, which may be compared with experimental data from real and simulated networks [6,7].

Complex networks describe many systems, most of which share three apparent features: power-law degree distribution, small average path length, and high clustering coefficient. With respect to their topology, they are usually divided into three large classes [8]: random networks, where all the nodes are randomly connected [9], scale-free network, where the number of links originating from a given node exhibits a power law distribution $p(k) \sim k^{-\gamma}$, with k being the degree (connectivity) of nodes [10], and the small-world one, showing structures where the diameter or the average shortest path ℓ increases logarithmically with the system size N [11].

Within the above context, Apollonian networks represent an important class of deterministic networks that are scale-free display small-world effect can be embedded in a Euclidean lattice and show space filling as well as matching graph properties [12,13]. Previous studies explored the topological features of Apollonian networks and their effect on the behavior of a variety of transport, growth, and Ising models [14–18]. Strongly correlated electrons on the Apollonian network were also studied showing an antiferromagnetic order and a metal-insulator transition [19]. Further, the spectral and thermodynamic behavior of a free-electron gas in the Apollonian network was investigated presenting several unique characteristics such as deltalike singularities, gaps, and minibands, as well as localized and extended electronic eigenstates [20]. These features were shown to be reflected in the thermodynamic behavior of the free-electron gas, particularly in the electronic specific heat [21].

On the other hand, the thermodynamic behavior of bosonic systems in complex networks is still unexplored. An underlying complex topology is expected to strongly affect the thermodynamic of the free-boson gas, particularly the Bose-Einstein condensation (BEC) phenomenon that leads to a macroscopic occupation of the ground state below a critical temperature. The effect of the network topology on the Bose-Einstein condensation has been the subject of recent investigations. The general conditions for the occurrence of BEC on networks in the presence of anomalous spectral regions in the density of states has been demonstrated [22–28]. Particularly, it was explained in detail the occurrence of BEC in the comb lattice which is obtained connecting to each site of a linear chain, namely, the backbone, a one-dimensional finger chain [24]. This lattice can be experimentally implemented as an array of Josephson junctions. Further, considering noninteracting bosons on a star network whose topology may be realized with a dilute atomic gas in a star-shaped deep optical lattice, Brunelli *et al.* showed the occurrence of a topology-induced BEC [25]. In this case, the ground state is localized around the star center, with the critical temperature depending only on the number of the star arms and on the Josephson energy of the bosonic Josephson junctions. However, the above networks are not complex, in the sense of not presenting power-law connectivity distribution and small average path length.

In this work, we address the open question concerning the thermodynamics of a bosonic gas with a conserved density distributed in a complex network. Due to its deterministic, scale-free, and small-world properties, the Apollonian network will be used as a prototype network. Within a tight-binding approach, we will show that a topology-induced Bose-Einstein condensation takes place with unconventional features directly related to the complex structure of the density of states. We will report the finite-size and density scaling behavior of the transition temperature and relate them to the fragmented structure of gaps and degeneracies of the energy spectrum. Further thermodynamic fingerprints of the underlying complexity will be shown in the specific-heat behavior.

We start by considering one bosonic particle moving on an Apollonian network described by a tight-binding Hamiltonian taking into account only hopping terms between directly connected sites of the network, namely,

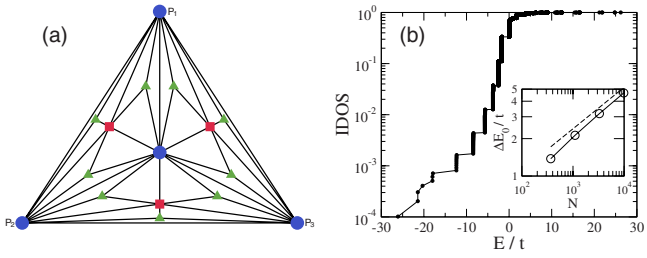

FIG. 1. (Color online) (a) Apollonian network with $g=3$. P_1, P_2, and P_3 are the sites of the original triangle at the zeroth generation. (b) IDOS within the tight-binding approximation for a single particle in an Apollonian network with $g=9$ generations. The vertical segments correspond to the degenerated energy levels while the horizontal segments are associated with the energy gaps. Observe in the inset the power-law scaling $\Delta E_0 \propto N^{1/3}$, where N is the total number of sites in a finite network.

$$H = \sum_n \epsilon_n |n\rangle\langle n| + \sum_{n,m}^{N} H_{nm} |n\rangle\langle m|. \tag{1}$$

Here $|n\rangle$ represents the state where the particle is localized at site n and ϵ_n is the on-site energy. Disregarding any source of inhomogeneity in the on-site potential, we will take $\epsilon_n=0$ without any loss of generality. The hopping amplitudes H_{nm} are non-null only between the connected sites of the network and will be taken as the only relevant microscopic energy scale ($H_{nm}=t$).

The Apollonian network in its simplest two-dimensional version starts with a single equilateral triangle. The construction proceeds recursively in terms of the generation g. For the $(g+1)$th generation, the network is obtained by inserting a node within each triangle of the gth generation and connecting it to each of the triangle corners [see Fig. 1(a)]. The total number of network nodes $N(g)=(3^g+5)/2$. This network has scale-free, small-world, and hierarchical properties, as well as a large clustering coefficient. Pictorial representations of the iteration process and details concerning the node and connectivity distributions can be found elsewhere [12–21].

Figure 1(b) depicts the integrated density of states (IDOS) for an Apollonian network with $g=9$ generations as obtained from the direct diagonalization of the Hamiltonian. The vertical segments correspond to the degenerated energy levels while the horizontal ones are associated with the energy gaps. The largest degeneracy is observed at $E=0$ which supports 1/3 of the one-particle states. The staircase aspect of IDOS reveals the discrete scale invariance of the energy spectrum. The inset shows that the energy gap between the ground and the first excited states presents a simple power-law scaling with the total number of nodes of the network, as $\Delta E_0 \propto N^{1/3}$. It implies in a diverging ground state energy when N increases. This scaling is associated with the divergent connectivity of the sites at the inner generations as the thermodynamic limit is approached. The ground state has a particle density distribution that decays as the site connectivity decreases. Therefore, in low temperatures, the bosons are predominantly localized on the sites of the first generations of the network. As the temperature increases, the excited states start to be populated and the bosons become more uniformly distributed on all network sites.

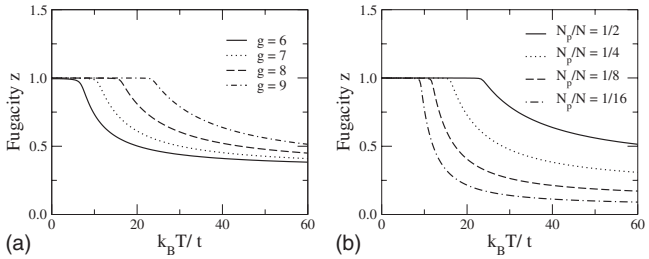

FIG. 2. (a) The fugacity as a function of temperature for Apollonian networks with distinct number of generations for $N_p/N=1/2$. Note the existence of a Bose-Einstein condensation at low temperature ($z \simeq 1$), which is rounded by finite-size effects. (b) The fugacity as a function of temperature for an Apollonian network with $g=9$ generations and different numbers of particles.

The thermodynamic behavior of a boson gas composed of a fixed number N_p of noninteracting bosons in an Apollonian network can be directly obtained from its energy spectrum. Both low- and high-temperature behavior are strongly affected by the constraint in the particle number. At low temperatures, a finite fraction of the particles may condensate at the ground state instead of just disappearing as it usually happens, for instance, with collective excitations in condensed matter. At high temperatures the internal energy saturates once new particles cannot be created and the energy spectrum is bounded.

Considering the grand canonical ensemble, the average number of particles at the ith energy state is defined by

$$\langle n_i \rangle = \frac{1}{z^{-1} \exp(\beta\varepsilon_i) - 1}. \tag{2}$$

Here $z=\exp(\beta\mu)$ is the fugacity, $\beta=1/k_BT$, and μ is the chemical potential which can be extracted from $N_p = \sum_{i=1}^{N} \langle n_i \rangle$.

In Fig. 2(a), we show the fugacity dependence on the temperature for the energy spectra generated from Apollonian networks with distinct generations and $N_p/N=1/2$. All energies were shifted by the ground state energy in order to have $\mu=0$ as the lower bound of the chemical potential. Note that the fugacity assumes values near unity at low temperatures, presenting a monotonic decay afterwards. In networks with a small number of generations, the transition from the low to the high-temperature regime is rounded by finite-size effects. It becomes singular only in the thermodynamic limit, representing the true Bose-Einstein transition. The present result shows that the transition temperature increases with the network size. For completeness, we plot in Fig. 2(b) the fugacity as a function of temperature for an Apollonian network with $g=9$ generations and different particle densities. The temperature dependence points to a Bose-Einstein condensation with a transition temperature that increases with the number of particles.

The average number of particles occupying the ground state, namely, N_0, can be directly obtained from the fugacity as $N_0=z/(1-z)$. We show in Fig. 3(a) the fraction of par-

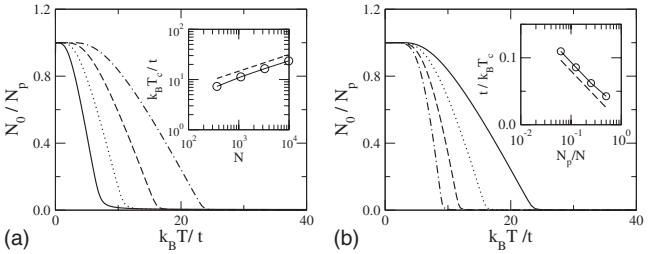

FIG. 3. (a) Fraction of particles N_0/N_p in the ground state as a function of temperature for networks with distinct number of generations: $g=6$ (solid line), $g=7$ (dotted line), $g=8$ (dashed line), and $g=9$ (dotted-dashed line). Here, we used the ratio $N_p/N=1/2$. The inset shows the dependence of transition temperature, T_c, on the total number of sites N of the network. The dashed line corresponds to $T_c \propto N^{1/3}$. (b) Fraction of particles N_0/N_p in the ground state as a function of temperature for an Apollonian network with $g=9$ generations and different number of particles: $N_p/N=1/2$ (solid line), $N_p/N=1/4$ (dotted line), $N_p/N=1/8$ (dashed line), and $N_p/N=1/16$ (dotted-dashed line). The inset show the dependence of the transition temperature T_c with the number of particles N_p/N. The dashed line corresponds to $N_p/N \propto \exp(-\epsilon'/k_BT_c)$.

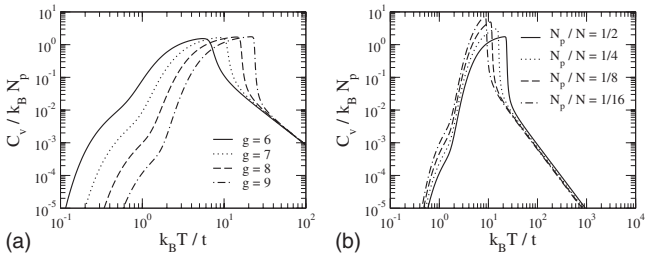

FIG. 4. The normalized specific heat as a function of temperature for noninteracting bosons in Apollonian networks: (a) considering networks with distinct generations and a fixed particle density; (b) considering a network with $g=9$ generations but different particle densities N_p/N. A discontinuity in the specific heat at the Bose-Einstein transition temperature develops as the thermodynamic limit is approached. The oscillations in the low-temperature behavior reflects the fragmented structure of the density of states.

ticles in the ground state N_0/N_p as a function of temperature for Apollonian networks with distinct generations, considering the ratio $N_p/N=1/2$. For low temperatures, the fraction N_0/N_p is finite. Except by the finite-size rounding off, the condensed fraction vanishes at a finite temperature which depends on the number of generations of the Apollonian network. We assume the temperature of maximum curvature as being the transition temperature T_c for a given finite network. The inset shows the dependence of transition temperature, T_c, on the total number of sites N of the network. The dashed line corresponds to the scaling behavior $T_c \propto N^{1/3}$, which reflects the size dependence of the gap between the ground and the first excited states. A proper rescaling of the hopping amplitudes would be required to obtain a finite transition temperature in the thermodynamic limit, as it is usually performed in lattice models with diverging connectivity.

Figure 3(b) depicts the fraction of particles condensed in the ground state as a function of temperature for an Apollonian network with $g=9$ generations and different particle densities. The transition temperature also increases with the particle density. However, it does not follow the power-law scaling usually observed in Bose-Einstein transitions. The inset shows the dependence of the inverse of the normalized transition temperature t/k_BT_c on the scaled number of particles N_p/N. Actually, the data can be well fitted by $N_p/N \propto \exp(-\epsilon'/k_BT_c)$, specially in the low-density regime. This behavior can be reproduced by assuming a simplified structure for the density of states composed of only two allowed energies: the ground state $\epsilon_0=0$ and a highly degenerated level with energy ϵ'. Within this scenario, the total number of particles can be written as $N_p=\Sigma_i[z^{-1}\exp(\beta\epsilon_i)-1]^{-1} \propto N\exp(-\epsilon'/k_BT_c)$, where it was assumed that at T_c there is a vanishing fraction of particles in the ground state, $z=1$ and $N_p/N \ll 1$.

Finally, we further explore the thermodynamic behavior of the present noninteracting boson gas on the Apollonian network by computing its specific heat. It is evaluated by differentiating the average internal energy $U(N,T)=\Sigma_{i=1}^{N}\varepsilon_i\langle n_i\rangle$ with respect to the temperature T, i.e., $C_v=dU(N,T)/dT|_V$, where V is the volume of the system which is kept constant by maintaining fixed the total number of one-particle accessible states N. It is straightforward to show that it can be put in the form

$$C_v/k_B = \frac{\sum_i \varepsilon_i^2 \sinh^{-2}(y_i) - \left[\sum_i \varepsilon_i \sinh^{-2}(y_i)\right]^2}{4(k_BT)^2 \sum_i \sinh^{-2}(y_i)}, \qquad (3)$$

with $y_i=(\varepsilon_i-\mu)/2k_BT$.

In Fig. 4(a), we show the normalized specific heat C_V/k_BN_p as a function of temperature for Apollonian networks considering distinct number of generations and a fixed particle density $N_p/N=1/2$. Note that the discontinuous jump at the Bose-Einstein transition temperature, usually depicted by trapped free-boson gases [29–32], is smoothened by finite-size effects. It only becomes a true discontinuity in the thermodynamic limit. The maximum value of the specific heat per particle does not depend on the network size. At high temperature, all curves merge into a single T^{-2} decay. The low-temperature behavior shows a modulation which is related to the fragmented structure of the energy landscape with several energy scales. Figure 4(b) shows the normalized specific heat C_V/k_BN_p as a function of temperature for the $g=9$ Apollonian network considering different particle densities. The maximum in the specific heat per particle decreases with increasing densities.

In summary, we determined the thermodynamic behavior of noninteracting bosons hopping in a deterministic complex network which exhibits scale-free and small-world characteristics. By considering a gas with a conserved density, we demonstrated that it displays a topology-induced Bose-Einstein condensation. This transition has a nature completely distinct from the BEC previously reported to occur in evolving complex networks associated with the capture of a macroscopic fraction of the links by a single node [33,34]. Here, we have a finite fraction of the particles condensing in the ground state of the network. Although the transition is

rounded off by finite-size effects, these become vanishingly small even for networks with a small number of generations, which allow to define an effective transition temperature on finite networks. We showed that the transition temperature increases with the network size as $T \propto N^{1/3}$, the same scaling shown by the gap between the ground and first excited states. The transition temperature has an anomalous dependence on the particle density which is related to the complex structure of gaps and degeneracies of the energy spectrum. The above features were also shown to be reflected in the temperature dependence of the specific heat. In principle, networks of Josephson junctions or optical networks could be used to probe the here proposed topological Bose-Einstein condensation. In these cases, effects of disorder and interparticle interactions should be taken into account. Further, the specific role played by the scale-free, small-world, and hierarchical properties of the network on the BEC transition can be explored by considering distinct topologies. It would be interesting to have future developments along these lines.

This work was partially financed by the Brazilian Research Agencies CAPES (Rede NanoBioTec), CNPq [INCT-Nano(Bio)Simes, Project No. 573925/2008-9], FAPERN/CNPq, FUNCAP/CNPq, and FAPEAL/CNPq (Pronex grants),

[1] R. Sharan and T. Ideker, Nat. Biotechnol. **24**, 427 (2006).
[2] S. Wassermann and K. Faust, *Social Network Analysis* (Cambridge University Press, Cambridge, 1994).
[3] R. Cohen, K. Erez, D. ben-Avraham, and S. Havlin, Phys. Rev. Lett. **85**, 4626 (2000).
[4] R. Cohen, K. Erez, D. ben-Avraham, and S. Havlin, Phys. Rev. Lett. **86**, 3682 (2001).
[5] A. A. Moreira, J. S. Andrade, and L. A. Nunes Amaral, Phys. Rev. Lett. **89**, 268703 (2002).
[6] H. Rozenfeld, J. Kirk, E. Bollt, and D. ben-Avraham, J. Phys. A **38**, 4589 (2005).
[7] E. Bollt and D. ben-Avraham, New J. Phys. **7**, 26 (2005).
[8] R. Albert and A.-L. Barabási, Rev. Mod. Phys. **74**, 47 (2002).
[9] P. Erdos and A. Rényi, Publ. Math. (Debrecen) **6**, 290 (1959).
[10] A.-L. Barabási and R. Albert, Science **286**, 509 (1999).
[11] D. J. Watts and H. Strogatz, Nature (London) **393**, 440 (1998).
[12] J. S. Andrade, H. J. Herrmann, R. F. S. Andrade, and L. R. da Silva, Phys. Rev. Lett. **94**, 018702 (2005).
[13] J. P. K. Doye and C. P. Massen, Phys. Rev. E **71**, 016128 (2005).
[14] R. F. S. Andrade and J. G. V. Miranda, Physica A **356**, 1 (2005).
[15] J. P. K. Doye and C. P. Massen, J. Chem. Phys. **122**, 084105 (2005).
[16] A. A. Moreira, D. R. Paula, R. N. Costa Filho, and J. S. Andrade, Phys. Rev. E **73**, 065101(R) (2006).
[17] R. F. S. Andrade and H. J. Herrmann, Phys. Rev. E **71**, 056131 (2005).
[18] R. F. S. Andrade, J. S. Andrade, Jr., and H. J. Herrmann, Phys. Rev. E **79**, 036105 (2009); C. N. Kaplan, M. Hinczewski, and A. N. Berker, *ibid.* **79**, 061120 (2009).
[19] A. M. C. Souza and H. J. Herrmann, Phys. Rev. B **75**, 054412 (2007).
[20] A. L. Cardoso, R. F. S. Andrade, and A. M. C. Souza, Phys. Rev. B **78**, 214202 (2008).
[21] I. N. de Oliveira, F. A. B. F. de Moura, M. L. Lyra, J. S. Andrade, Jr., and E. L. Albuquerque, Phys. Rev. E **79**, 016104 (2009).
[22] R. Burioni, D. Cassi, I. Meccoli, M. Rasetti, S. Regina, P. Sodano, and A. Vezzani, Europhys. Lett. **52**, 251 (2000).
[23] R. Burioni, D. Cassi, M. Rasetti, P. Sodano, and A. Vezzani, J. Phys. B **34**, 4697 (2001).
[24] P. Buonsante, R. Burioni, D. Cassi, and A. Vezzani, Phys. Rev. B **66**, 094207 (2002).
[25] I. Brunelli, G. Giusiano, F. P. Mancini, P. Sodano, and A. Trombettoni, J. Phys. B **37**, S275 (2004).
[26] T. Matsui, Infinite Dimen. Anal., Quantum Probab., Relat. Top. **9**, 1 (2006).
[27] P. Sodano, A. Trombettoni, P. Silvestrini, R. Russo, and B. Ruggiero, New J. Phys. **8**, 327 (2006).
[28] P. Silvestrini, R. Russo, V. Corato, B. Ruggiero, C. Granata, S. Rombetto, M. Russo, M. Cirillo, A. Trombettoni, and P. Sodano, Phys. Lett. A **370**, 499 (2007).
[29] V. Bagnato, D. E. Pritchard, and D. Kleppner, Phys. Rev. A **35**, 4354 (1987).
[30] S. Grossmann and M. Holthaus, Phys. Lett. A **208**, 188 (1995).
[31] R. K. Pathria, Phys. Rev. A **58**, 1490 (1998).
[32] N. Sandoval-Figueroa and V. Romero-Rochín, Phys. Rev. E **78**, 061129 (2008).
[33] G. Bianconi and A.-L. Barabási, Phys. Rev. Lett. **86**, 5632 (2001).
[34] L. Ferretti and G. Bianconi, Phys. Rev. E **78**, 056102 (2008).